Quasi-Ballistic Transport Model for Graphene Field-Effect Transistor

Guangxi Hu, *Member, IEEE*, Shuyan Hu, Ran Liu, Lingli Wang, *Member, IEEE*, Xing Zhou, *Senior Member, IEEE*, and Ting-Ao Tang, *Senior Member, IEEE*

***Abstract*— Based on McKelvey's flux theory, a carrier transport model for a graphene field-effect transistor (GFET) is addressed. This model leads to an explicit expression for drain-to-source current with only a few fitting parameters. The model is verified with experiments and simulations, and good agreements are observed. With the model, the characteristics of drain-to-source current of the GFET with positive or negative gate biases can be obtained very quickly and easily. The model will provide some insights and guidance for the practical use of the GFETs and can be embedded in circuit simulation tools.**

***Index Terms*— Field-effect transistor (FET), graphene, modeling, quasi-ballistic transport.**

I. Introduction

As METAL–OXIDE–SEMICONDUCTOR field-effect transistor (MOSFET) continues to scale down, graphene seems to be one of the most favorable materials for the channel in FETs in the near future. With the advantages of its high mobility, excellent chemical and mechanical stabilities, and 2-D structure, graphene shows a perspective usage. Experimental researches were conducted intensively on those transistors where graphene was used as channel material [1]–[3]. Meric *et al.* [1] showed that graphene FET (GFET) can be used in analog and radio-frequency circuits. To facilitate the wide applications of GFET, analytical models for drain current, transconductance, threshold voltage, and cutoff frequency are highly needed. The drain current model is one of the most important. Thiele *et al.* [4] used a quasi-analytical modeling approach to calculate the current–voltage (I–V) characteristics. Jiménez and Moldovan [5] used drift-diffusion carrier transport approach to obtain an explicit drain current model. Wang *et al.* [6] presented a virtual-source I–V model. Though the aforementioned drain current models agreed well with experiments, they all included many fitting parameters and were in a rather complicated form, thus it is inconvenient for applications.

Manuscript received January 29, 2013; revised May 3, 2013; accepted May 15, 2013. Date of current version June 17, 2013. This work was supported by the Special Funds for Major State Basic Research, China 973 Project under Grant 2006CB302703. The review of this paper was arranged by Editor A. C. Seabaugh.

G. Hu, R. Liu, L. Wang, and T.-A.Tang are with the State key laboratory of ASIC & system, School of microelectronics, Fudan University, Shanghai 200433, China (e-mail: gxhu@fudan.edu.cn).

S. Hu is with the School of electronics and information, Tongji University, Shanghai 200092, China.

X. Zhou is with the School of electrical and electronic engineering, Nanyang Technical University, 639798 Singapore.

Color versions of one or more of the figures in this paper are available online at http://ieeexplore.ieee.org.

Digital Object Identifier 10.1109/TED.2013.2264094

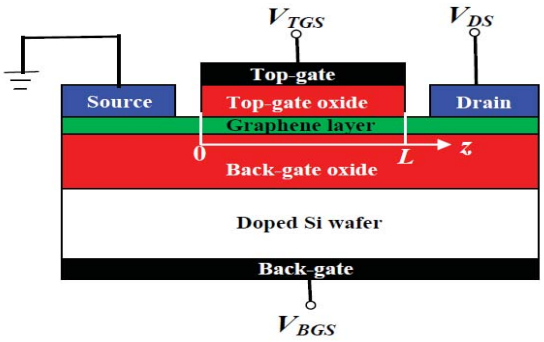

Fig. 1. Sketch map of a double-gate (DG) GFET.

In this paper, we use McKelvey's flux theory [7] and quasi-ballistic transport model (BTM) to obtain an explicit analytical drain current expression for GFETs. The analytical results match with the experimental and simulated results quite well, and also the model is in a simplified form, including only a few fitting parameters. The BTM is used in the studies of double-gate (DG) and nanowire MOSFET, where the channel material is silicon [8], [9]. We use this approach to investigate the surrounding-gate MOSFET, and obtain a unified carrier transport model, which is applicable in both ballistic- and diffusive-transport regimes [10].

II. Drain Current Model

The sketch of a GFET is shown in Fig. 1, where a layer of graphene with a channel length L, and a channel width W, is placed on a back-gate oxide. The channel length and width are along the z- and x-directions (not shown in the figure). The biases applied to the top gate, back gate, and the drain are $V_{\rm TGS}$, $V_{\rm BGS}$, and V_{DS}, respectively, and the electric potential at the source is referenced to zero.

The directed fluxes in a GFET can be understood from [10]. The beginning of the channel is defined at the location of virtual cathode, where the electric potential reaches to its minimum or the barrier height for electrons reaches to the top. We define flux as, in this paper, the carriers pass through the channel per unit width per second, and in the units of $\rm m^{-1}s^{-1}$.

The drain-to-source current, I_{DS}, is given by charges carried by net fluxes between the positive- and the negative-going fluxes as follows:

$$I_{DS} = Wq\left[F^{+}(0) - F^{-}(0)\right] \tag{1}$$

where q is the elementary charge, $F^+(0)$ and $F^-(0)$ are positive- and negative-going carrier fluxes, respectively.

The source-injected fluxes, $F^+(0)$ can be expressed as [10] follows:

$$F^+(0) = \sum_{k_x} \sum_{k_z>0} n^+(0)\, \bar{v}_z \tag{2}$$

where $n^+(0)$ is the carrier sheet density associated with $F^+(0)$ and $\bar{v}_z$ is the average velocity of the injected carriers. According to the theory of density-of-states (DOS) [11], the total number of quantum states per unit area in the 2-D graphene is $g_D k^2/(2\pi)$, where g_D is the valley degeneracy factor and is 2. For a large area of graphene, the dispersion relationship between the energy and the wave vector, k, is in a linear form near the K point [12], then the 2-D DOS is expressed as $D_2(E) = 2(E - E_C)/\pi(\hbar v_F)^2$, where E_C is conduction band energy, v_F is the Fermi velocity, and $v_F = 9.71 \times 10^5$ m/s [11]. The summations in (2) can be replaced with an integral over energy, using Fermi statistics, we obtain the following:

$$\begin{aligned} F^+(0) &= \frac{1}{2}\int_{E_C}^{\infty} D_2(E)\, f(E)\, \bar{v}_z dE \\ &= \frac{\bar{v}_z}{\pi\hbar^2 v_F^2}\int_{E_C}^{\infty} \frac{E - E_C}{\exp\left(\frac{E-E_F}{k_B T}\right)+1} dE. \end{aligned}$$

The factor 1/2 rises from $k_z > 0$. Finishing the integral, leading to the following:

$$F^+(0) = \bar{v}_z (k_B T/\hbar v_F)^2 \zeta_1(\eta_F)/\pi \tag{3}$$

where $\zeta_1(\eta_F) = \int_0^{\infty} x dx/[\exp(x - \eta_F) + 1]$ is the Fermi integral, $\eta_F = (E_F - E_C)/k_B T$, $E_F = qV_{CH}$, V_{CH} is the voltage drop across the quantum capacitance [4], and $\hbar$, k_B, and T have their usual meanings.

With the same method, the negative-directed fluxes at the drain end can be obtained as follows:

$$F_b^-(L) = F^+(0)\, \zeta_1(\eta_F - U_{DS})/\zeta_1(\eta_F) \tag{4}$$

where $U_{DS} = qV_{DS}/k_B T$.

In the presence of scattering, the negative-going fluxes at the source end, $F^-(0)$, are composed of two parts [9], [10]: $rF^+(0)$ and $(1-r)F_b^-(L)$, with r being the backscattering coefficient. Hence, we have the following:

$$F^-(0) = rF^+(0) + (1-r)F_b^-(L). \tag{5}$$

The carriers' sheet density at the beginning of the channel is [10] $n(0) = [F^+(0) + F^-(0)]/v_F$. Then, $F^+(0)$ and $F^-(0)$ can be solved by substituting them into (1), the drain current is as follows:

$$I_{DS} = \frac{qWv_F n(0)(1-r)[1 - \zeta_1(\eta_F - U_{DS})/\zeta_1(\eta_F)]}{1 + r + (1-r)\zeta_1(\eta_F - U_{DS})/\zeta_1(\eta_F)}. \tag{6}$$

To obtain I_{DS}, $n(0)$ is needed, which is expressed as [4], [5] as follows:

$$n(0) = KV_{CH}^2/(2q) + n_i \tag{7}$$

where $K = (2q^3/\pi)/(\hbar v_F)^2$, n_i is the induced carrier sheet density [5] and is treated as a fitting parameter, and V_{CH} is given by [4], [5] the equation shown at the bottom of this page, where $V_{\mathrm{T,eff}} = V_{\mathrm{TGS}} - V_{\mathrm{TGS},0} - V$ and $V_{\mathrm{B,eff}} = V_{\mathrm{BGS}} - V_{\mathrm{BGS},0} - V$ are the effective voltages applied to the top and the back gates, respectively, and V is the voltage drop in the graphene channel, which is zero at the source end and V_{DS} at the drain end. $V_{\mathrm{TGS},0}$, and $V_{\mathrm{BGS},0}$ are introduced to consider the work function difference between the gate material and the graphene, and for the charges at the graphene/oxide interface [4]. The values of $V_{\mathrm{TGS},0}$ and $V_{\mathrm{BGS},0}$ can be obtained from the measured I–V curves [2], which correspond to the current minima. C_{Tox} and C_{Box} are the capacitances per unit area of the top and the back oxides, respectively. $C_{\mathrm{Tox}} = \varepsilon_{ox}/t_{\mathrm{Tox}}$, and $C_{\mathrm{Box}} = \varepsilon_{ox}/t_{\mathrm{Box}}$, where t_{Tox} (t_{Box}) is the thickness of the top (back) oxide, and ε_{ox} is the permittivity of the oxide.

To compare model results with experimental data, source/drain (S/D) contact resistances need to be considered, and thus V_{DS} in (6) should be replaced with an effective drain bias, V_{DS}^{eff}, which is given by $V_{DS}^{\mathrm{eff}} = V_{DS}^{\mathrm{app}} - I_{DS}(R_S + R_D)$, where V_{DS}^{app} is the bias actually applied to the drain, and R_S and R_D are the S/D resistances, respectively. The voltage applied to the graphene channel is now actually smaller than that applied to the drain. To obtain an explicit expression for I_{DS}, as well as to avoid solving the coupled drain-voltage and drain-current equations iteratively, we model V_{DS}^{eff} as $V_{DS}^{\mathrm{eff}} = (1-\beta)V_{DS}^{\mathrm{app}}$, where β is a fitting parameter and its value depends on S/D contact resistances and drain biases.

Similar to [8], the backscattering coefficient, r, is defined and evaluated as $r = \ell/(\ell + \lambda)$, where λ is the low field momentum relaxation length, and ℓ is critical scattering length which is expressed as follows:

$$\ell = L(\delta/U_{DS})^{\alpha}. \tag{9}$$

Equation (9) is introduced based on a larger gate length and/or a smaller drain bias will result in a smaller electric field along the channel direction, and the critical scattering length will be larger, leading to a larger backscattering coefficient and a smaller drain current. The detailed discussions on critical scattering length can be found in [8]. δ and α are the fitting parameters introduced to adjust the influence of gate length and drain bias on the backscattering coefficient, hence the model results can best fit experiments or simulations.

Similar to the treatment in [8] and [10], we model λ as $\lambda = 2\mu k_B T/(\theta q v_F)$, where μ is the carrier mobility, whose low-field value can be obtained from experiments, and θ is a

$$V_{CH} = \frac{\sqrt{(C_{\mathrm{Tox}} + C_{\mathrm{Box}})^2 + 2K\left[V_{T,eff}C_{\mathrm{Tox}} + V_{B,eff}C_{\mathrm{Box}}\right]} - (C_{\mathrm{Tox}} + C_{\mathrm{Box}})}{K} \tag{8}$$

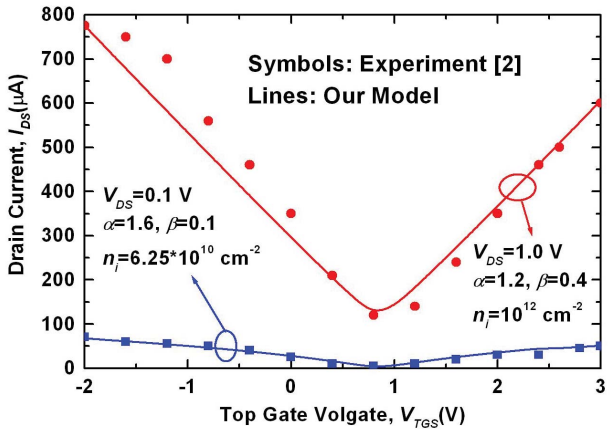

Fig. 2. Transfer characteristics of a GFET. Symbols: experimental results. Solid line: results of this model. $L = 10$ μm, $W = 5$ μm, $t_{\rm Tox} = 40$ nm, $\varepsilon = 16\varepsilon_0$, $V_{\rm TGS,0} = 0.85$ V, $V_{B,eff} = 0$ V, $\mu = 800$ cm^2/V $\cdot$ s, $\delta = 0.8$, and $\theta = 1$. Experimental data are mapped from [2, Fig. 3].

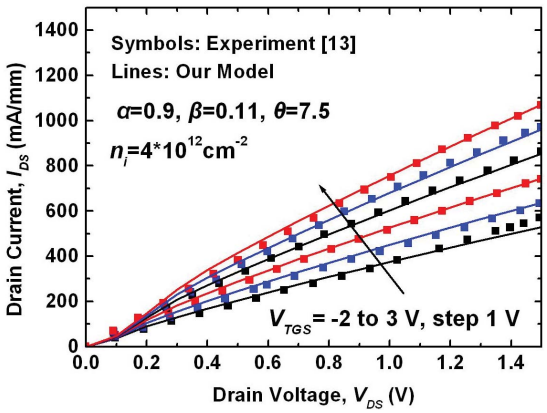

Fig. 3. Output characteristics of a GFET. Squares: experimental results [13, Fig. 1C]. Solid lines: results of this model. $L = 240$ nm, $W = 30$ μm, $C_{\rm Tox} = 0.195$ μF/cm^2, $C_{\rm Box} = 0$, $\mu = 1000$ cm^2/V $\cdot$ s, $V_{\rm TGS,0} = -3.6$ V, $V_{B,eff} = 0$, $\alpha = 0.9$, $\beta = 0.11$, $\theta = 7.5$, $\delta = 0.8$, and $n_i = 4 \times 10^{12}$ cm^{-2}.

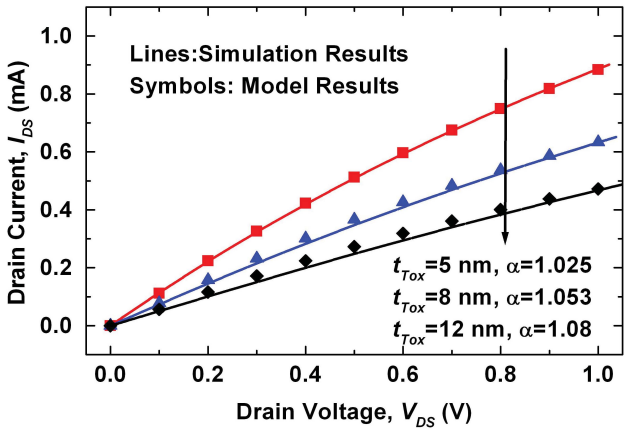

Fig. 4. Drain currents of the GFETs with different top-gate oxide thickness. $L = W = 1$ μm, $t_{\rm Box} = 300$ nm, $V_{T,eff} = 0.6$ V, $V_{\rm TGS,0} = 0$, $V_{B,eff} = 0$, $\beta = 0$, $\delta = 0.8$, $\theta = 1$, $\mu = 3000$ cm^2/V$\cdot$ s, and $n_i = 0$. Solid lines: results obtained with simulations. Symbols: results of this model.

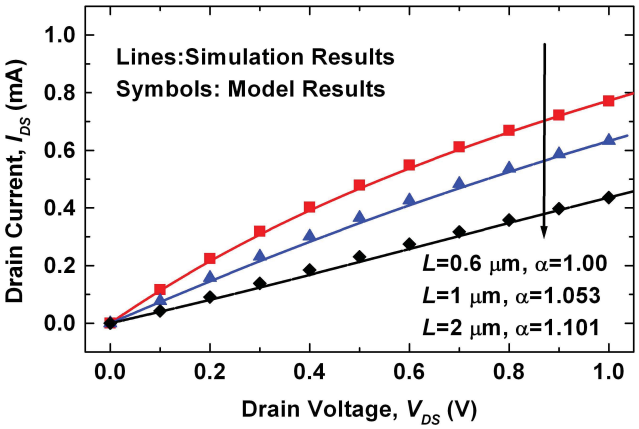

Fig. 5. Drain currents of the GFETs with different channel length. $t_{\rm Tox} = 8$ nm, $t_{\rm Box} = 300$ nm, $W = 1$ μm, $V_{T,\rm eff} = 0.6$ V, $V_{\rm TGS,0} = 0$, $V_{B,\rm eff} = 0$, $\beta = 0$, $\delta = 0.8$, $\theta = 1$, $\mu = 3000$ cm^2/V$\cdot$ s, and $n_i = 0$. Solid lines: results obtained with simulations. Symbols: results of this model.

fitting parameter used to adjust the mobility value for the high electric fields.

III. Verifications

Initially, we compare model results with experiments reported in [2, Fig. 3]. According to the experiment, the parameters are: $V_{\rm TGS,0} = 0.85$ V, $V_{B,eff} = 0$, $L = 10$ μm, $W = 5$ μm, $t_{\rm Tox} = 40$ nm, $\varepsilon_{ox} = 16\varepsilon_0$, and ε_0 is the permittivity in the vacuum. We choose $\mu = 800$ cm^2/V$\cdot$ s, the value of which falls into the range of the experiment, $\theta = 1$. The GFET is biased for two different drain voltages: $V_{DS} = 0.1$ V and $V_{DS} = 1.0$ V. When we choose the appropriate values for the fitting parameters α, β, δ, and n_i, we can capture the V-shaped behavior of the drain current. The model results match with those of experiments quite well, as shown in Fig. 2.

Then, we compare our model results with experiments [13, Fig. 1C] where the GFET channel length is only 240 nm. According to [13] and its supplemental material, the parameters are: $C_{\rm Tox} = 0.195$ μF/cm^2, $W = 30$ μm, $C_{\rm Box} = 0$, $n_i = 4 \times 10^{12}$ cm^{-2}, $V_{\rm TGS,0} < -3.5$ V, $V_{B,\rm eff} = 0$, and the low-field mobility ranges between 800 and 1600 cm^2/V $\cdot$ s. We set $V_{\rm TGS,0} = -3.6$ V and $\mu = 1000$ cm^2/V$\cdot$ s accordingly. The calculated output characteristics for the range of $V_{\rm TGS}$ from -2 to 3 V are shown in Fig. 3. When $\alpha = 0.9$, $\beta = 0.11$, $\delta = 0.8$, and $\theta = 7.5$ are assumed, all the results agree very well except for very small V_{DS} (<0.2 V). Under a small V_{DS}, the backscattering coefficient, r, is exaggerated a little, and the model results are underestimated to some extent, leading to the small discrepancies between the model and the experiments.

Finally, we test our model against a known simulation tool, GFET tool from nanoHUB, the code of that uses the drift-diffusion approach to calculate the I–V behavior of the GFET, self-consistently with the temperature of the device [14]. The parameters used in the simulations are: $\mu = 3000$ cm^2/V$\cdot$ s, $t_{\rm Box} = 300$ nm, $V_{B,\rm eff} = 0$ (no back-gate bias is applied), $V_{\rm TGS,0} = 0$, and very small S/D contact resistances (1 $\Omega\cdot$ μm^2) are chosen deliberately to ignore their influences. Default values are used for other parameters. The material for the dielectrics of the top and back gates is silicon dioxide. The parameters used in our model are: $\beta = 0$, $\delta = 0.8$, $\theta = 1$, and $n_i = 0$.

The simulated and modeled drain currents of the devices with different t_{Tox} and different L are shown in Figs. 4 and 5, respectively, and very good agreement between the simulation and the modeling is observed.

IV. Conclusion

So far, a drain current model for GFET was presented and developed for the first time using McKelvey's flux theory and quasi-BTM theory. S/D resistances were considered and only a few fitting parameters were used. Model devices with different geometries and biases were tested against experiment and simulation results, and good agreements were observed.

Our model results fitted well with experiments for the device with both a long ($L = 10$ μm, [2]) and a short ($L = 240$ nm, [13]) channel. As our model was developed from that addressed in [8], and as stated in [8], the model was based on fundamental physical reasoning, it worked well. As shown in Fig. 2, our model can capture the V-shaped I–V characteristics of the GFET, with electrons transporting for positive gate biases and holes transporting for negative gate biases.

In the numerical computation, when V_{DS} was large (> 0.5 V), (6) can be replaced with the following equation, which can be used for fast circuit simulations.

$$I_{DS} = \frac{qWv_F n\,(0)\,(1-r)\left[1-\exp(-U_{DS})\right]}{1+r+(1-r)\exp(-U_{DS})}. \tag{10}$$

In practical applications, integrated circuit (IC) designers needed the I–V characteristics of the GFET device in circuit simulation and circuit design. The explicit and rather simple expression for the drain current presented in this paper is suitable for the model to be used and embedded in circuit simulation tools to facilitate the development of GFET-based IC in the future.

V. Discussions

In the practical use of the model, the values of fitting parameters, α, β, θ, δ, and n_i need to be chosen, to which we give some guidance here.

The fitting parameters α and δ are associated with backscattering coefficient, r. For a long-channel device, the coefficient r should be large but it is sometimes overestimated. The fitting parameters α and δ should be chosen to adjust r to an appropriate value.

The fitting parameter β is mostly determined by the S/D contact resistances. In addition, β is also determined by channel length and drain bias to some extent. Because for short-channel devices, and/or under large drain bias, the drain current will be large, the voltage drop across the S/D will also be large, hence the voltage actually applied to the graphene channel will be small, and thus the value of fitting parameter β should be large.

The fitting parameter θ is used to adjust the mobility value. The low-field mobility value can be obtained from experiments, but sometimes a high-field mobility value is needed in simulations. θ is thus used to adjust the mobility to an appropriate value in the high-field region, as well as to accommodate the different mobility values for electrons and holes. As the value of high-field mobility is always smaller than the low field, the value of parameter θ is always > 1 and it falls into the ranges between 1 and 10.

The fitting parameter n_i can be obtained as the following: at a zero-effective gate bias, tune n_i to such an extent that the model drain current best fits with current minimum of the experiment.

The value of the thickness of the top-gate oxide does not affect the accuracy of the model, as shown in Fig. 4, neither does the value of the thickness of the back-gate oxide. As the back-gate oxide usually has a large thickness (> 300 nm) and a small capacitance, from (8) we know that its influence on the drain current is very small and can be neglected, therefore, the variation of the thickness of the back-gate oxide has little to do with the accuracy of the model.

As we use the constant mobility and a simplified model for the voltage drop across the S/D, our drain current model has some limitations: 1) it only works in the linear region and it cannot capture the saturation behavior and 2) the value of fitting parameters should be changed from device to device.

References

[1] I. Meric, M. Y. Han, A. F. Young, B. Ozyilmaz, P. Kim, and K. Shepard, "Current saturation in zero-bandgap, top-gated graphene field-effect transistors," *Nature Nanotechnol.*, vol. 3, no. 11, pp. 654–659, 2008.

[2] J. Kedzierski, P.-L. Hsu, A. Reina, J. Kong, P. Healey, P. Wyatt, and C. Keast, "Graphene-on-insulator transistors made using C on Ni chemical-vapor deposition," *IEEE Electron Device Lett.*, vol. 30, no. 7, pp. 745–747, Jul. 2009.

[3] W. J. Liu, X. W. Sun, Z. Fang, Z. R. Wang, X. A. Tran, F. Wang, L. Wu, G. I. Ng, J. F. Zhang, J. Wei, H. L. Zhu, and H. Y. Yu, "Positive bias-induced V_{th} instability in graphene field effect transistors," *IEEE Electron Device Lett.*, vol. 33, no. 3, pp. 339–341, Mar. 2012.

[4] S. A. Thiele, J. A. Schaefer, and F. Schwierz, "Modeling of graphene metal-oxide-semiconductor field-effect transistors with gapless large-area graphene channels," *J. Appl. Phys.*, vol. 107, no. 9, pp. 094505-1–094505-8, May 2010.

[5] D. Jiménez and O. Moldovan, "Explicit drain-current model of graphene field-effect transistors targeting analog and radio-frequency applications," *IEEE Trans. Electron Devices*, vol. 58, no. 11, pp. 4049–4052, Nov. 2011.

[6] H. Wang, A. Hsu, J. Kong, D. A. Antoniadis, and T. Palacios, "Compact virtual-source current-voltage model for top- and back-gated graphene field-effect transistors," *IEEE Trans. Electron Devices*, vol. 58, no. 5, pp. 1523–1533, May 2011.

[7] J. P. McKelvey, R. L. Longini, and T. P. Brody, "Alternative approach to the solution of added carrier transport problems in semiconductors," *Phys. Rev.*, vol. 123, no. 1, pp. 51–57, Jul. 1961.

[8] A. Rahman and M. S. Lundstrom, "A compact scattering model for the nanoscale double-gate MOSFET," *IEEE Trans. Electron Devices*, vol. 49, no. 3, pp. 481–489, Mar. 2002.

[9] M. Lundstrom, Z. Ren, and S. Datta, "Essential physics of carrier transport in nanoscale MOSFETs," *IEEE Trans. Electron Devices*, vol. 49, no. 1, pp. 133–141, Jan. 2002.

[10] G. Hu, J. Gu, S. Hu, Y. Ding, R. Liu, and T.-A. Tang, "A unified carrier-transport model for the nanoscale surrounding-gate MOSFET comprising quantum-mechanical effects," *IEEE Trans. Electron Devices*, vol. 58, no. 7, pp. 1830–1836, Jul. 2011.

[11] G. W. Hanson, *Fundamentals of Nanoelectronics*. Upper Saddle River, NJ, USA: Pearson Education, Inc., 2008.

[12] T. Fang, A. Konar, H. Xing, and D. Jena, "Carrier statistics and quantum capacitance of graphene sheets and ribbons," *Appl. Phys. Lett.*, vol. 91, no. 9, pp. 092109-1–092109-3, Aug. 2007.

[13] Y.-M. Lin, C. Dimitrakopoulos, K. A. Jenkins, D. B. Farmer, H.-Y. Chiu, A. Grill, and P. H. Avouris, "100-GHz transistors from wafer-scale epitaxial graphene," *Science*, vol. 327, no. 5966, p. 662, Feb. 2010.

[14] E. Pop and F. Lian. (2011). *GFET Tool* [Online]. Available: http://nanohub.org/resources/gfettool

Guangxi Hu (M'07) received the Ph.D. degree from Fudan University, Shanghai, China.

His current research interests include semiconductor device physics, multigate MOSFETs, and nanoscale MOSFETs modeling and simulation.

Shuyan Hu is currently pursuing the B.S. degree with the School of electronics and information, Tongji University, Shanghai, China.

Ran Liu received the Ph.D. degree from the Max-Planck-Institute for Solid State Research, Germany, in 1990.

He is a Cheung Kong Chair Professor with Fudan University, Shanghai, China.

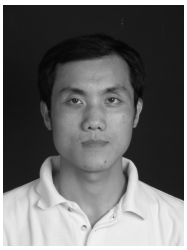

Lingli Wang (M'99) received the Ph.D. degree in electrical engineering from Napier University, Edinburgh, U.K., in 2001.

His current research interests include logic synthesis, reconfigurable computing, and quantum computing.

Xing Zhou (S'88–M'91–SM'99) received the Ph.D. degree in electrical engineering from the University of Rochester, Rochester, NY, USA, in 1990.

His current research interests include semiconductor device physics and modeling, compact model development for advanced devices.

Ting-Ao Tang (M'93–SM'03) received the B.S. Degree from the Physics Department, Fudan University, Shanghai, China, in 1961.

He is a Professor with the Department of Microelectronics, Fudan University.